Inter-annual variability of summertime CO_2 exchange in Northern Eurasia inferred from GOSAT XCO_2

2016 Environ. Res. Lett. 11 105001

(http://iopscience.iop.org/1748-9326/11/10/105001)

IOP Publishing Environ. Res. Lett. 11 (2016) 105001 doi:10.1088/1748-9326/11/10/105001

Environmental Research Letters

CrossMark

OPEN ACCESS

RECEIVED
29 February 2016

REVISED
10 August 2016

ACCEPTED FOR PUBLICATION
7 September 2016

PUBLISHED
28 September 2016

LETTER

Inter-annual variability of summertime CO_2 exchange in Northern Eurasia inferred from GOSAT XCO_2

M Ishizawa[1], K Mabuchi[1], T Shirai[1], M Inoue[1,4], I Morino[1], O Uchino[1], Y Yoshida[1], D Belikov[1,2,3] and S Maksyutov[1]

[1] National Institute for Environmental Studies, Tsukuba, Japan
[2] Tomsk State University, Tomsk, Russia
[3] National Institute of Polar Research, Tachikawa, Japan
[4] Present address: Akita Prefectural University, Akita, Japan.

E-mail: ishizawa.misa@nies.go.jp

Keywords: carbon cycle, climate variability, inverse modeling, satellite-based observations

Abstract

Northern Eurasia is one of the largest terrestrial carbon reservoirs on the Earth's surface. However, since the coverage of surface CO_2 observations is still limited, the response to the climate variability remains uncertain. We estimated monthly CO_2 fluxes for three sub-regions in Northern Eurasia (north of ~60°N), Northeastern Europe, Western Siberia and Eastern Siberia, using CO_2 retrievals from the Japanese Greenhouse Gases Observing SATellite (GOSAT). The variations of estimated CO_2 fluxes were examined in terms of the regional climate variability, for the three consecutive growing seasons of 2009–2011. The CO_2 fluxes estimated using GOSAT data are highly correlated with the surface temperature anomalies in July and August ($r > 0.8$) while no correlation is found in the CO_2 fluxes estimated only using surface observations. The estimated fluxes from GOSAT data exhibit high negative correlations with one-month lagged positive precipitation anomalies in late summer ($r > -0.7$) through surface temperature and the Normalized Difference Vegetation Index (NDVI). The results indicate that GOSAT data reflects the changes in terrestrial biospheric processes responding to climate anomalies. In 2010, a large part of Eurasia experienced an extremely hot and dry summer, while cold and wet weather conditions were recorded in Western Siberia. The CO_2 fluxes estimated from GOSAT data showed a reduction of net CO_2 uptake in Northeastern Europe and Eastern Siberia, but the enhancement of net CO_2 uptake in Western Siberia. These opposite sub-regional flux anomalies can be explained by the different climate anomalies on a sub-regional scale in Northern Eurasia. Thus, this study demonstrates that space-based observations by GOSAT compensate for the lack of ground-based observational coverage so as to better capture the inter-annually varying atmosphere-terrestrial biosphere CO_2 exchange on a regional scale.

1. Introduction

Northern Eurasia is one of the largest terrestrial carbon reservoirs on the Earth's surface. Its response to climate change is of concern, especially in light of the vulnerability of permafrost under the ongoing global warming (Zimov *et al* 2006, McGuire *et al* 2009). Despite the importance of Northern Eurasia for the climate system and the global carbon cycle, the ground-based measurements are still limited. The top-down CO_2 flux estimates in Northern Eurasia are poorly resolved (e.g. Chevallier *et al* 2010). To compensate the spatial limitation of the current surface greenhouse gases observation network, satellite measurement projects have been initiated. As a first greenhouse gases-dedicated satellite, the Greenhouse Gases Observing SATellite (GOSAT) was launched in January 2009 by the National Institute for Environmental Studies (NIES), the Japan Aerospace Exploration Agency (JAXA) and the Ministry of the Environment (MOE) (Kuze *et al* 2009). The column-averaged dry-air mole fractions of CO_2 (XCO_2) are retrieved from the Short-Wavelength InfraRed (SWIR) spectra obtained by onboard Thermal And

Near infrared Sensor for carbon Observation-Fourier Transform Spectrometer (TANSO-FTS) (Yoshida *et al* 2011). GOSAT observes globally, but the coverage of GOSAT XCO_2 varies seasonally mainly with solar zenith angle. In northern high latitudes, GOSAT XCO_2 is available in the non-winter seasons, from late spring to early autumn. Even for the limited period, GOSAT XCO_2 retrievals have a potential to improve understanding of the regional CO_2 fluxes in far north regions.

Atmospheric CO_2 inversion is the approach to optimize surface fluxes through minimizing the differences in atmospheric CO_2 concentration between the measurements and model simulation (e.g. Enting and Newsam 1990, Enting 2002, Peylin *et al* 2013). It is expected in principle that the increase in atmospheric CO_2 measurements (observational constraints) can help improve the CO_2 flux estimates. In particular, satellite-based measurements, such as GOSAT data, hold potential because of much more availability in spatial coverage than ground-based measurements (Rayner and O'Brien 2001, Chevallier *et al* 2009). On the other hand, it is still necessary and challenging to evaluate how the increase of measurement coverage improves CO_2 flux estimates (e.g. Gloor *et al* 2000, Bruhwiler *et al* 2011, Mabuchi *et al* 2016). GOSAT data have been used to estimate CO_2 sources and sinks in several studies (e.g. Basu *et al* 2013, Maksyutov *et al* 2013, Saeki *et al* 2013, Chevallier *et al* 2014, Deng *et al* 2014). Most of these GOSAT inversion studies examined the CO_2 flux distribution on a global scale and demonstrated considerable uncertainty reduction in estimated fluxes compared to the inversions with traditional ground-based measurements only. The objectives of this study are to utilise GOSAT data focusing on the regional flux estimates in Northern Eurasia, and evaluated how variations of the GOSAT-estimated fluxes are consistent with possible underlying processes. The question we investigated is how the GOSAT XCO_2 can detect sub-regional CO_2 flux anomalies. For this, we examined the inter-annual variations of GOSAT-estimated summertime CO_2 fluxes for 2009–2011 in terms of the response of the terrestrial biosphere in Northern Eurasia to the climate anomalies on a regional scale. Guerlet *et al* (2013) reported lower summertime drawdown of GOSAT XCO_2 in 2010 than 2009 over North America and Eurasia, and estimated 0.89 $\pm$ 0.20 GtC reduction of CO_2 uptake in Eurasia possibly due to the heat wave. Compared to Guerlet *et al* (2013) that studied on a continental scale, this study focuses on the sub-regional scale monthly CO_2 fluxes in Northern Eurasia for the three years of growing season, 2009–2011, including the year 2010 when an extremely hot summer was experienced in Northern Europe. Our study is the first attempt to evaluate the GOSAT inverted fluxes for Northern Eurasia with the environmental drivers (surface temperature and precipitation) and the independent index of terrestrial biospheric productivity, NDVI. We discuss how GOSAT XCO_2 data can improve the detectability of CO_2 flux signal on the response of the land–atmosphere CO_2 exchange to the climate variability on a regional scale.

2. Methods

To estimate the regional CO_2 fluxes for 2009–2011, we conducted the following two global inversions, using an inverse modeling system based on the Global Eulerian-Lagrangian Coupled Atmospheric Model (GELCA). The first is the joint inversion, in which GOSAT XCO_2 was used from June 2009 in addition to ground-based CO_2 observations. The second is the surface inversion with ground-based CO_2 observations only. Both inversion calculations were started from 2001 with ground-based observational data only until the GOSAT XCO_2 became available in June 2009. By starting the inversion much earlier than the period of our period of interest, we can avoid the initialization problem of the model atmospheric CO_2 concentration field that may cause artifact emissions or sources. The details of GELCA inversion modeling system can be found in Shirai *et al* (2016) and Ishizawa *et al* (2016). In the following sections, we briefly describe the framework of GELCA inverse modeling, the prior CO_2 fluxes, and observational data.

2.1. GELCA inverse modeling

GELCA is a coupled atmospheric model of National Institute for Environmental Studies-Transport Model (NIES-TM) version 8.1i, and FLEXPART version 8.0 (Ganshin *et al* 2012). FLEXPART (Stohl *et al* 2005) is a Lagrangian particle dispersion model, which provides the finer footprint information near the observational sites. FLEXPART releases 10 000 particles from the observation points and simulates them backward in time for 2 days. At the end points, the time-varying background CO_2 concentration levels are given by NIES-TM (Belikov *et al* 2013) which is a Global Eulerian model with a horizontal resolution of 2.5° × 2.5°. Both FLEXPART and NIES-TM are driven by the meteorological fields from the Climate Data Assimilation System of the Japan Meteorological Agency (JCDAS) (Onogi *et al* 2007) with a spatial resolution of 1.25° × 1.25° and a temporal resolution of 6 h. Kalman Smoother optimization technique was employed with a fixed lag of 3 months (Bruhwiler *et al* 2005) to estimate monthly CO_2 fluxes over 42 land and 22 ocean regions on the globe. The region mask used in this study is identical to the one for NIES-GOSAT Level 4 CO_2 products (Maksyutov *et al* 2013). Figure 1 shows the three Northern Eurasian sub-regions of interest in this study.

2.2. Prior fluxes

The prior CO_2 fluxes used to predict CO_2 concentrations consist of four components: 1) fossil fuel

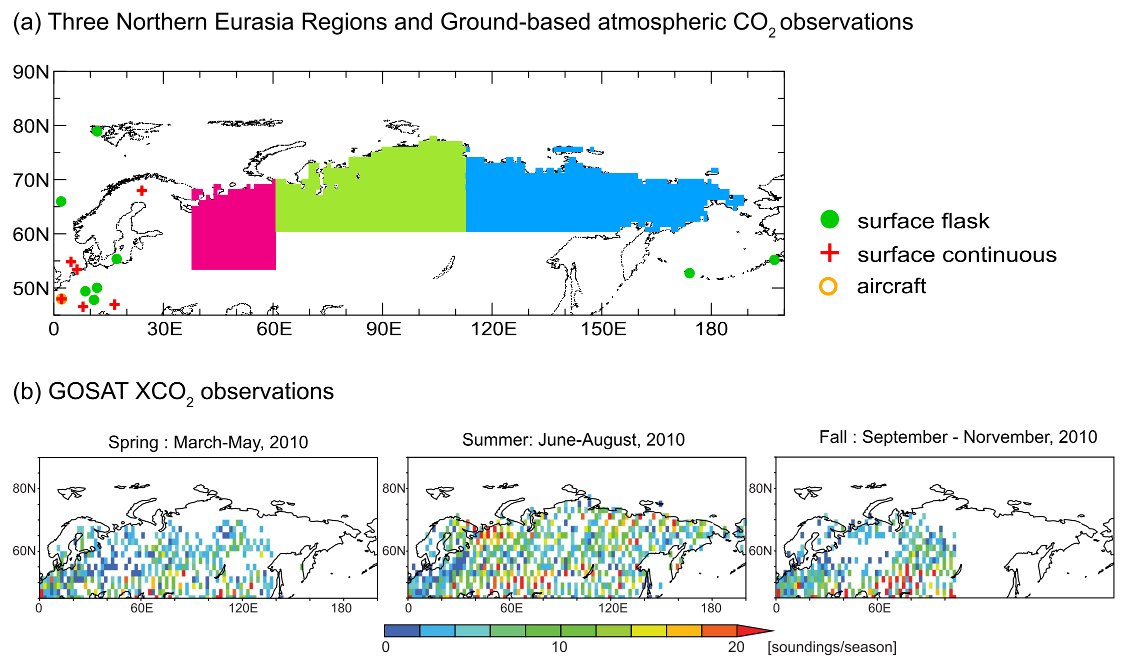

Figure 1. Three northern Eurasia regions considered in this study and locations of CO_2 and XCO_2 observations in our inversion. (a) three regions: Northeastern Europe (red), Western Siberia (yellow-green) and Eastern Siberia (light blue). The ground-based atmospheric CO_2 observation sites are shown in different markers by sampling type or platform. All the sites are located outside of the three northern Eurasia regions. (b) Locations of XCO_2 observed by GOSAT are shown here by the number of sounding over $2° \times 2°$ grid in spring, summer and fall in 2010. In winter, no GOSAT data cover the above three Northern Eurasia regions.

emission inventory of the Open source Data Inventory of Anthropogenic CO_2 (ODIAC) (Oda and Maksyutov 2011), 2) net ecosystem CO_2 exchange from a process-based terrestrial biosphere model, the Vegetation Integrative Simulator for Trace gases (VISIT) (Ito 2010, Saito *et al* 2014), 3) the ocean-atmosphere CO_2 exchange from the Offline ocean Tracer Transport Model (OTTM) (Valsala and Maksyutov 2010), and 4) the biomass burning CO_2 emission of Global Fire Emission Database (GFED) version 3.1 (van der Werf *et al* 2010). VISIT terrestrial biospheric fluxes are at a daily time step; other fluxes are in monthly temporal resolution. All of them are on $1.0° \times 1.0°$ grid.

2.3. Observations

2.3.1. GOSAT XCO_2

We used NIES GOSAT SWIR Level 2 XCO_2 (version 02.11). NIES GOSAT project team has been retrieving the XCO_2 with 'full physics approach', by which the optical path length modification due to aerosol scattering is connected with several aerosol parameters in the forward model. XCO_2 retrievals are subject to aerosol parameter and other settings in the retrieval algorithm, and suffer from systematic biases. Comparisons of GOSAT XCO_2 with the ground-based XCO_2 at 13 sites of Total Carbon Column Observing Network (TCCON) revealed that the NIES GOSAT XCO_2 has a negative bias of 1.48 ppm with a standard deviation of 2.09 ppm (Yoshida *et al* 2013). To minimize the systematic error in GOSAT XCO_2, we corrected possible biases of GOSAT XCO_2, using a multiple linear regression to the same version of GOSAT XCO_2 (v02.11) and simultaneously retrieved auxiliary parameters (aerosol optical depth, surface pressure, surface albedo, airmass) against TCCON XCO_2 retrievals (Inoue *et al* 2016). The GOSAT soundings over lands are observed in high and medium modes. Over oceans, sun-glint mode is used due to the low reflectance of ocean surface except for sun-glint direction. These three modes exhibit different characteristics of their retrieval biases. Since land XCO_2 in the medium gain (which is used over bright desert surfaces) have not been enough validated by TCCON XCO_2, we used high gain XCO_2 for lands and ocean sun-glint XCO_2 after being bias-corrected. In the inverse modelling, the data uncertainty of 2.31 ppm is assigned uniformly based on the global mean standard deviation (SD) of the difference between TCCON XCO_2 and its co-located single shot GOSAT-XCO_2, and the mean SD of XCO_2 at TCCON stations (station bias) (Yoshida *et al* 2013). The temporal coverage of GOSAT measurements are shown in figure 1. Summer is the season most covered by GOSAT, while there is no GOSAT observation available in winter.

2.3.2. Ground-based CO_2 observations

We used the Observation Package (ObsPack) data product v.1.0.3 (available at www.esrl.noaa.gov/gmd/ccgg/obspack) (Masarie *et al* 2014) provided by the National Oceanic and Atmospheric Administration

(NOAA) the Earth System Research Laboratory (ESRL), as ground-based atmospheric CO_2 concentrations. The ObsPack product consists of surface data obtained by a number of institutes and agencies as well as NOAA/ESRL global network. Figure 1 shows the locations of ground-based CO_2 measurement sites around Northern Eurasia that we used in this study. It is noted that there is no measurement site within the regions of interest in this study. The data uncertainties for the inverse modelling are assigned individually to the measurement sites based on the mean residual standard deviations from smooth curves, provided by GLOBALVIEW-CO_2 (2011). The minimum uncertainty is set to 0.25 ppm followed by Gurney *et al* (2004).

3. Meteorological parameters and NDVI

In this study, we examine the correlations of estimated CO_2 fluxes with three meteorological parameters (surface temperature, shortwave radiation, precipitation) and the Normalized Difference Vegetation Index (NDVI). These meteorological parameters are important factors in controlling the terrestrial biosphere processes, and then to impact the CO_2 exchange between the land and atmosphere (e.g. Mabuchi 2013)). NDVI is calculated from the visible and near-infrared lights reflected by vegetation. NDVI is closely linked with green cover, vegetation primary production, and phenology (Tucker 1979, Myneni *et al* 1995). A high value of NDVI indicates healthy or dense vegetation with high photosynthetic activity while a low value of NDVI indicates unhealthy or sparse vegetation with low photosynthetic activity. Since NDVI provides a measure of the condition and dynamics of vegetation in the lands, it could help evaluate the estimated CO_2 fluxes.

Surface temperature data used in this study are obtained from the JCDAS data set that is also used as a driving parameter for GELCA. We used daytime mean shortwave radiation and NDVI which are processed by JAXA from the spectral radiances obtained by the MODerate resolution Imaging Spectroradiometer (MODIS) on the NASA Earth Observing System satellites, Terra and Aqua (Saigusa *et al* 2010) (data available at http://kuroshio.eorc.jaxa.jp/JASMES/). The precipitation data are from the Climate Prediction Center Merged Analysis of Precipitation (CMAP) (Xie and Arkin 1997). The CMAP is global monthly analyses of precipitation which is produced by merging the ground-based observations from rain gauges and several satellite-based estimates. To highlight the relationship between inter-annual variations of estimated monthly surface CO_2 fluxes and climate anomalies, we obtained the monthly anomalies of above parameters, subtracting the respective means for 2009–2011 that is the period of the interest in this study.

4. Results and discussion

4.1. Temporal variations of estimated CO_2 fluxes

The time-series of estimated CO_2 fluxes in the three regions of Northern Eurasia are shown in figure 2. Differences of estimated CO_2 fluxes between the surface inversion and the joint inversion are seen in the summer months, showing the GOSAT XCO_2 data mainly impact in summer months in the northern high latitudes.

Besides larger summertime CO_2 uptake by joint inversion rather than surface inversion, in Northeastern Europe, it is noticeable that the summer 2010 uptake by joint inversion was quite reduced compared with 2009 and 2011. Similar reduction of summer 2010 uptake is also seen in Eastern Siberia, but not in Western Siberia. In Western Siberia, on the contrary, the joint inversion infers larger CO_2 uptake in 2010 than 2009. Furthermore, the joint inversion in 2010 infers much larger CO_2 uptake than the surface inversion though both inversion results are comparable in 2009 and 2011. This year-to-year change in the estimated CO_2 flux for Western Siberia is opposite to the results for Northeastern Europe and Eastern Siberia.

In this study, we focus on the anomalies of estimated CO_2 fluxes. Since the systematic retrieval biases of XCO_2 significantly affect the flux estimates, it is challenging to estimate the absolute value of the regional-scale CO_2 fluxes. The satellite-based inversion tends to infer larger summertime net CO_2 uptake in Northeastern Europe than surface inversion (e.g., (Chevallier *et al* 2014, Reuter *et al* 2014, Houweling *et al* 2015)). Though the magnitude of CO_2 fluxes has not been solved fully yet, the relative variations of CO_2 fluxes in time and space appear to be robust.

4.2. Correlations of estimated CO_2 fluxes with climate and NDVI anomalies

Before examining the correlation between estimated CO_2 fluxes and climate, and NDVI, we look at the spatial patterns of the inter-annual and intra-annual variations in the climate and NDVI anomalies in the summer seasons for 2009 to 2011.

Figure 3 shows the summertime mean (June–August) anomalies of surface temperature as a deviation of the mean temperature of 2009–2011. In 2010, it is noticeable that the temperature anomalies are positive in East Northeastern Europe and Siberia while negative in West Western Siberia. The anomaly patterns of 2009 and 2010 are overall opposite to each other. The 2011 anomaly varies spatially but appears to be relatively moderate as a whole, compared to the preceding two years.

Monthly anomalies of surface temperature, shortwave radiation, precipitation and NDVI in the summer of 2010 are shown in figure 4. In July, Northeastern Europe and Eastern Siberia show highly positive surface temperature anomalies. This anomaly

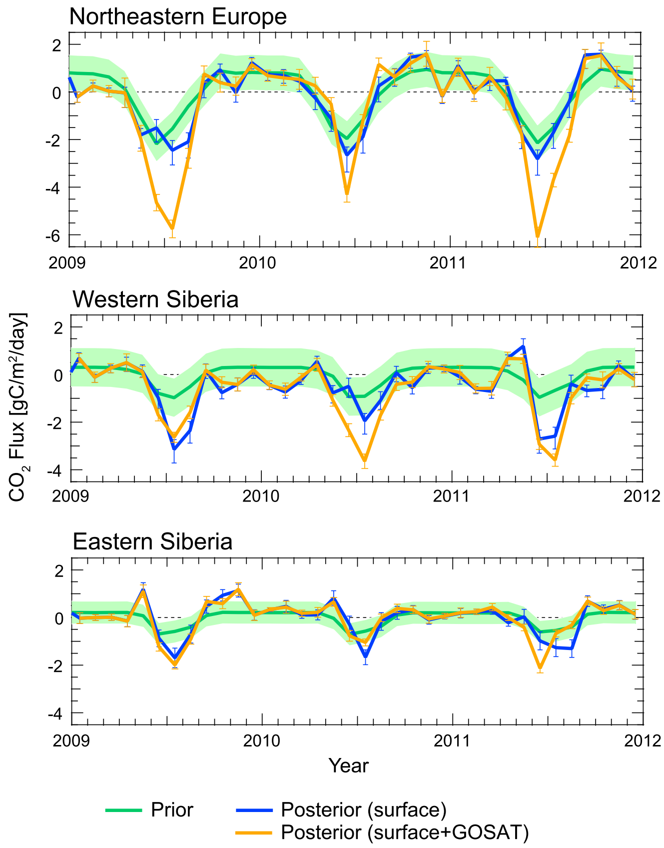

Figure 2. Monthly CO_2 flux estimates in the three regions of figure 1. Surface and joint inversion results are in blue and orange lines, respectively. Prior fluxes are shown in green curves with uncertainty of green-shaded. A negative flux is a flux from the atmosphere to the terrestrial biosphere.

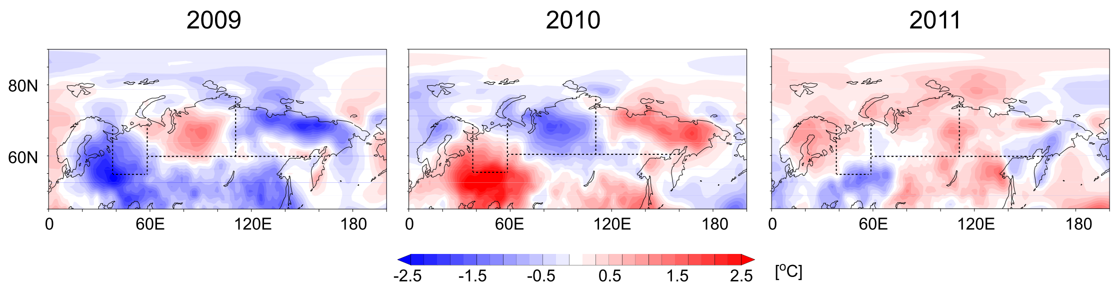

Figure 3. Summertime (June–August) averaged surface air temperature anomaly from the JCDAS dataset. The anomalies are calculated as the deviation from three-year monthly mean for 2009–2011. The boundaries for the three Northern Eurasia regions are indicated in dotted lines.

pattern is persistent in August and appears in the summertime mean pattern as seen in figure 3. In Western Siberia, the temperature anomaly remains negative in the entire summer of 2010. The spatial patterns of shortwave radiation are relatively similar to temperature as they are highly correlated by ($r = 0.83$). Precipitation anomaly patterns are fundamentally opposite to temperature ($r = -0.45$) and shortwave radiation ($r = -0.76$) due to the effects of cloud and soil moisture. The climate anomaly impacts on terrestrial vegetation activities, resulting in an NDVI anomaly. NDVI does not necessarily change spontaneously with climate as there is a time lag for the vegetation to respond to the climate change. It is thus important to see the temporal evolution of NDVI with climate change. The NDVI anomaly in Western Siberia is negative in June and becomes gradually positive from July to August. On the other hand, the NDVI anomaly in Northeastern Europe remains negative in the whole summer and its magnitude gradually increases from June through to August. The NDVI anomaly in Eastern Siberia is positive in June and becomes gradually negative from July to August. It indicates that the hot and dry conditions in the summer of 2010 suppress the vegetation activities in Northeastern Europe and Eastern Siberia. On the contrary, the cool and wet

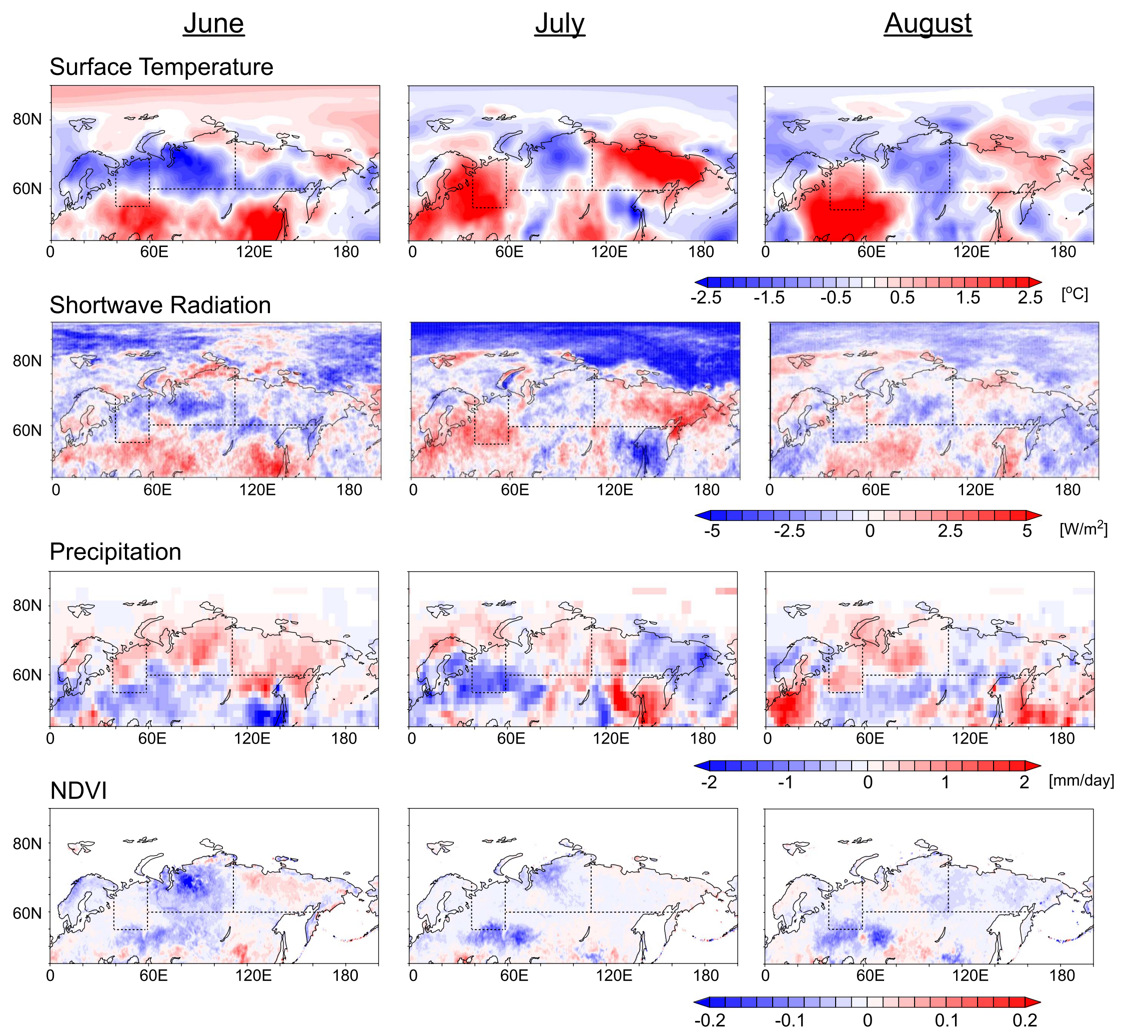

Figure 4. Monthly anomalies of surface temperature, shortwave radiation, precipitation and NDVI over Northern Eurasia for the year of 2010. The respective anomalies are calculated as their deviations from the 2009–2011 averaged monthly means. The boundaries for the three Northern Eurasia regions are indicated in dotted lines.

conditions in Western Siberia keep the vegetation green and photosynthetically active in August.

Figure 5 shows the correlations of CO_2 flux anomalies of both joint and surface inversions with the anomalies of surface temperature, shortwave radiation, and NDVI. The net CO_2 flux is a balance between the downward flux (negative) by photosynthetic activity and upward fluxes (positive) through ecosystem respiration. The positive net CO_2 flux means the respiration exceeds the photosynthesis. During the summer months, June to August, the estimated CO_2 fluxes are negative in all the three Northern Eurasian regions (as seen in figure 2), that is, these land regions exert net CO_2 uptake. Then the negative CO_2 flux anomalies indicate the increase of net CO_2 uptake by land ecosystems. In contrast, the positive CO_2 flux anomalies indicate the reduction of net CO_2 uptake. Overall, the CO_2 flux anomalies of both inversions are reasonably correlated with the anomalies of surface temperature, shortwave radiation, and NDVI. In the following sections, we examine the details.

4.2.1. Surface temperature

In June, both surface and joint inversion show a negative correlation. In July and August, joint inversion shows that strong positive correlations between temperature and CO_2 flux anomalies of 0.88 and 0.82, respectively, although no correlation is found in the surface inversion. In general, for the terrestrial ecosystems in the northern high latitudes, warmer weather in spring and early summer stimulates photosynthetic activities and the growth of vegetation, resulting in an increase of net CO_2 uptake by the terrestrial biosphere. In the middle and late summer, hotter weather conditions increase soil respiration, leading to an increase in CO_2 release from the land surface to the atmosphere. As a result, the net CO_2 uptake is reduced. This mechanism accounts for the change of the correlation between CO_2 flux anomalies of joint inversion and temperature anomalies, from negative correlation in June to positive correlation in July and August. Furthermore, the better correlations of CO_2 flux anomalies of joint inversion indicate that GOSAT

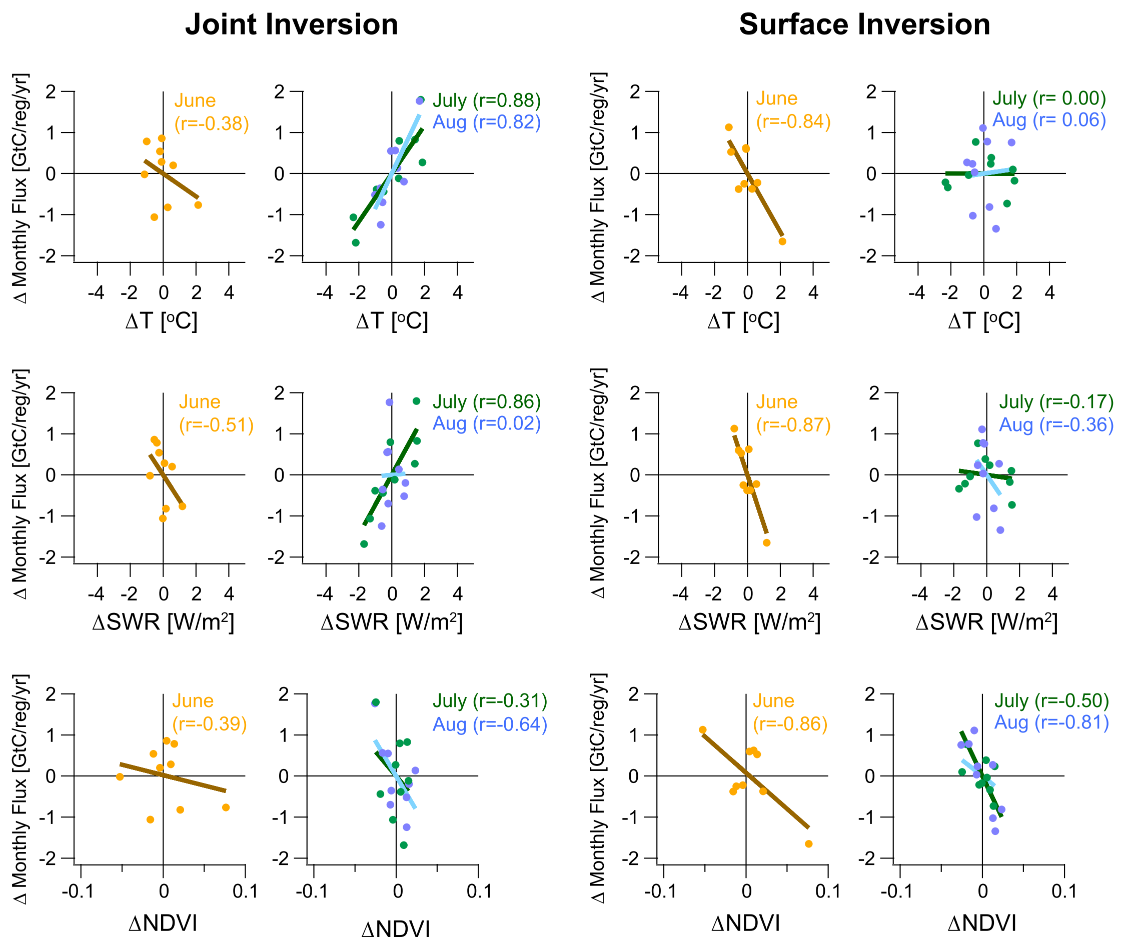

Figure 5. Monthly correlations between estimated CO_2 flux anomalies and the anomalies of surface temperature (top), shortwave radiation (middle) and NDVI (bottom), for June–August, 2009–2011. The anomalies of estimated CO_2 fluxes are from joint inversion (left) and surface inversion (right). Solid lines refer to the linear regression lines for June (orange), July (green), August (light blue), and the respective correlation coefficients (r) are shown in the plots. Individual regional anomalies are deviations from the respective regional monthly means for the same three years of 2009–2011. Correlations between anomalies were calculated over all three northern Eurasia regions together.

XCO_2 reflects well the land–atmosphere CO_2 exchange varying with surface temperature.

In the summer of 2010, a large part of Eurasia experienced an extremely hot and dry summer, though in Western Siberia the temperature anomalies were negative (cold) and the precipitation anomalies were positive (wet) over the summer months (see figures 3 and 4). The joint inversion shows reduced net CO_2 uptake in Northeastern Europe and Eastern Siberia (shown in figure 2), but enhanced net CO_2 uptake in Western Siberia. This regional difference in flux anomalies is consistent with the temperature dependency of net CO_2 flux anomaly discussed above, given the spatial variations of temperature anomalies in the summer of 2010. Cooler weather conditions in Western Siberia caused the negative CO_2 flux anomalies while Northeastern Europe and Eastern Siberia, which experienced the extreme hotter summer, yielded positive CO_2 flux anomalies.

From the difference of GOSAT XCO_2 data between 2009 and 2010, Guerlet *et al* (2013) estimated the 2010 summertime reduction of CO_2 uptake over Eurasia as a whole and attributed the CO_2 uptake reduction to the extremely hot weather conditions around Northern Europe. However, the extreme climate anomaly in July and August 2010 did not happen uniformaly over the entire Eurasia continent; the climate anomalies are spatially different on a sub-regional scale as seen in figure 4. Our GOSAT-inferred fluxes corresponded to such sub-regional scale differences in temperature anomalies (figure 2). The correlation analysis endorses the relationship between the surface temperature and net CO_2 fluxes in the joint inversion.

4.2.2. Shortwave radiation

As for the joint inversion, the correlations of CO_2 flux anomalies with shortwave radiation anomalies in June and July are similar to the correlations with temperature anomalies, though there is no correlation in August. On the other hand, the surface inversion shows small but negative correlation in August, indicating the increase of net CO_2 uptake with shortwave radiation.

Shortwave radiation has effects to the terrestrial biosphere directly and indirectly. As a control factor of photosynthesis, shortwave radiation enhances the photosynthetic activity and then increases carbon CO_2 uptake. In addition, as the major driver to increase the surface temperature, shortwave radiation impacts on biospheric processes through the surface temperature. Moreover, shortwave radiation increases transpiration which reduces soil moisture, but also moderates surface temperature increase.

The negative correlations for June in both joint and surface inversions might be results of both direct and indirect effects of shortwave radiation on the terrestrial processes, that is, the enhancement of photosynthetic activity by shortwave radiation, and also the favorably warm weather conditions for plant growth through the increase of surface temperature as seen in section 4.2.1.

The joint inversion shows a positive correlation with shortwave radiation in July. This positive correlation can be explained by the indirect effect of shortwave radiation. The shortwave radiation increases surface temperature, and results in the increase of ecosystem respiration as seen in section 4.2.1. On the other hand, no correlation is seen for August in the joint inversion. The relationship between CO_2 flux and shortwave radiation through the indirect effect (change in surface temperature) is influenced by soil moisture. Surface temperature is not always proportional to shortwave radiation. Plenty of soil moisture would hamper the rise of surface temperature as shortwave radiation energy is more partitioned into latent heat to evaporate soil water than sensible heat. Thus, the interaction with shortwave radiation and soil moisture may complicate the correlation between shortwave radiation anomalies and CO_2 flux anomalies for joint inversion in August. The soil moisture is considered to be mainly controlled by precipitation with a time-lag. We examine the impact of precipitation anomalies on CO_2 fluxes later in section 4.2.4.

4.2.3. NDVI

During the summer months, the CO_2 flux anomalies of both joint and surface inversion show negative correlations with NDVI anomalies. These results are consistent with the fact that positive NDVI anomalies indicate healthier vegetation, which is capable of taking up more CO_2 from the atmosphere through photosynthesis, potentially leading to negative net CO_2 flux anomalies. The CO_2 fluxes from surface inversion appear to be correlated more strongly with NDVI anomalies than those from joint inversion. This stronger negative correlation of surface inversion is consistent with the negative correlation with shortwave radiation for the entire summer as discussed in the previous section. A positive shortwave anomaly could increase the photosynthesis response, and result in a positive NDVI anomaly. From two decadal NDVIs and climate data analysis, Nemani *et al* (2003) indicated that solar radiation is limiting factor of carbon net anomaly in the northern vegetation. On the other hand, the weaker negative correlation between NDVI and joint inversion might indicate the complex response of terrestrial biosphere to climate anomalies. NDVI is a proxy of biospheric productivity but is not necessary to increase linearly net CO_2 uptake. In the next section, we examine further the relationship between CO_2 flux and NDVI anomaly regarding the relationship with precipitation and the biospheric processes.

4.2.4. Precipitation

The same month anomalies between precipitation and CO_2 fluxes show no clear correlation (not shown), except the negative correlation between joint inversion and precipitation anomalies for July ($r = -0.78$). Among the same month anomalies of meteorological parameters and NDVI, precipitation appears not to be correlated with NDVI, while precipitation has weak negative correlations with shortwave radiation and surface temperature, except high correlation with surface temperature in July ($r = -0.71$).

It is considered that the precipitation controls the soil water. Through the soil water/soil moisture, the precipitation anomaly impacts on biospheric processes, and then on land–atmosphere CO_2 exchanges. This interaction is not necessarily spontaneous, but relativity slow. Therefore, we examined the precipitation anomalies with a time delay. The positive correlations were found between the precipitation anomalies in early spring and the NDVI anomalies for the early growing season with one to three-month lag (not shown). Among them, the precipitation anomalies in July show high correlations with the anomalies of surface temperature and NDVI in August. Figure 6 shows the precipitation anomalies in July correlated negatively with surface temperature anomalies in August ($r = -0.76$) and positively with the NDVI anomalies in August ($r = 0.56$). The negative correlation between the one-month delayed precipitation anomaly and temperature anomaly are consistent with the temperature rise by shortwave radiation being suppressed by soil moisture.

In figure 6, the CO_2 flux anomalies in August are plotted on the top of the correlation plots between the precipitation anomalies in July and the surface temperature anomalies/NDVI anomalies in August. As seen in figure 6, one-month lagged precipitation anomalies are highly correlated with surface temperature negatively ($r = -0.76$) and NDVI positively ($r = 0.56$), though those same month correlations are relatively weak for surface temperature ($r = -0.45$) and no correlation is found with NDVI as mentioned earlier. The CO_2 anomaly values are drawn by color and size of the closed circles. The results indicate that the CO_2 flux anomalies from joint inversion are more clearly related to one-month delayed precipitation anomalies and same month anomalies of surface temperature and NDVI. These relationships can be summarised as follows:

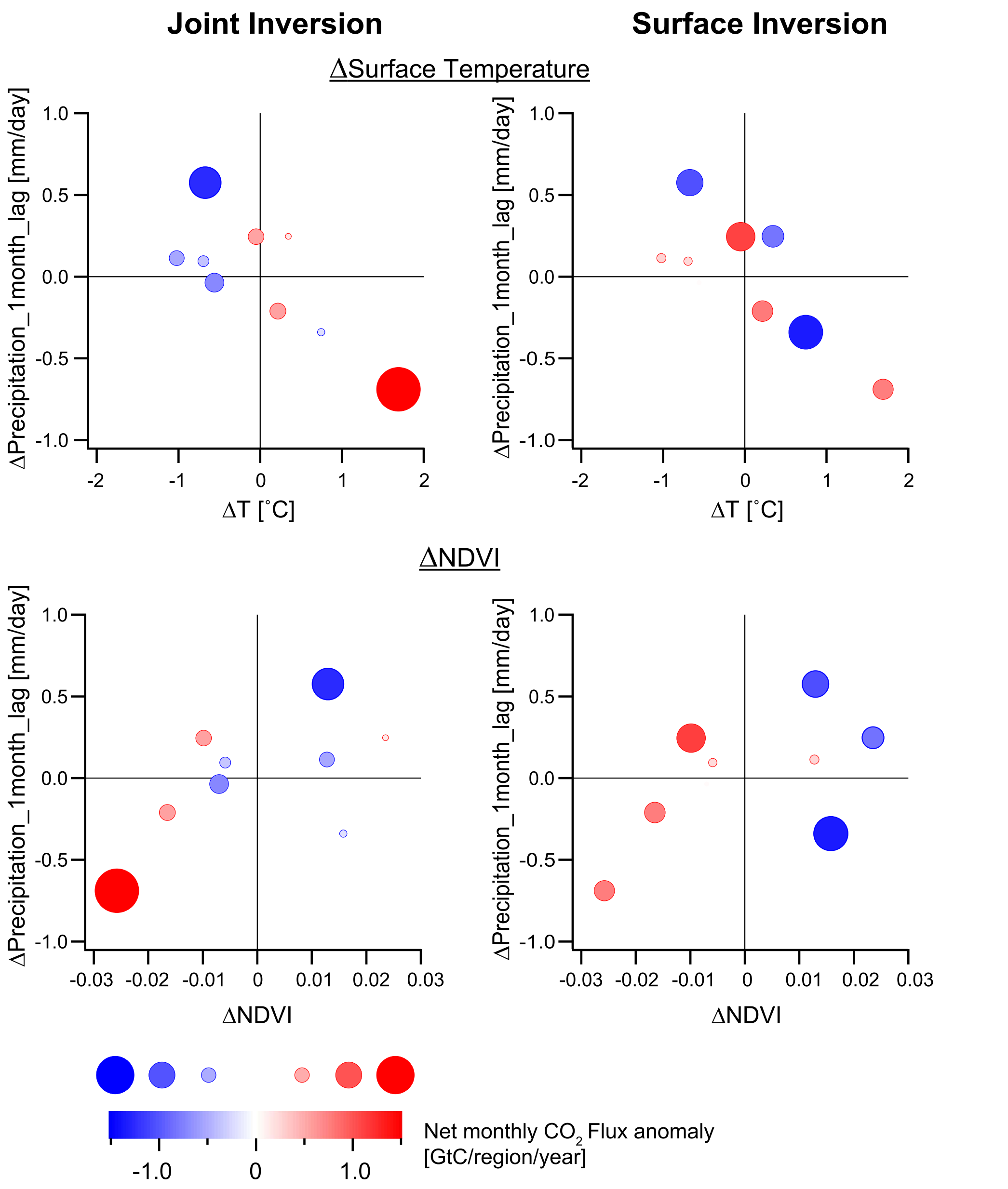

Figure 6. Correlations between surface temperature anomaly in August and precipitation anomaly in July (top), and between NDVI anomaly in August and precipitation anomaly in July (bottom), for 2009–2011. The color and size of the closed circles denote the corresponding monthly CO_2 flux anomalies in August.

- Negative CO_2 flux anomalies with lower temperature and more previous-month precipitation (a cooler condition with wet soil).
- Positive CO_2 flux anomalies with higher temperature and less previous-month precipitation (a hotter condition with dry soil).
- Negative CO_2 flux anomalies with higher NDVI and more previous-month precipitation (healthy vegetation with wet soil condition).
- Positive CO_2 flux anomalies with lower NDVI and less previous-month precipitation (unhealthy vegetation with dry soil condition).

The above relationships indicate that the precipitation in July is key for the land–atmosphere CO_2 exchange in August; the precipitation of July supplies soil moisture and then support the photosynthetic process also affects the soil respiration by controlling the surface temperature (surface condition) through energy exchange between land and atmosphere. This combined effect of climate and NDVI on the net CO_2 uptake is consistent with previous studies on the warming effect of northern vegetation (e.g. Barber *et al* 2000, Angert *et al* 2005, Ma *et al* 2012).

Recent studies on the terrestrial biosphere response in the northern hemisphere to climate change conclude the vegetation greening and increasing carbon uptake in the spring in northern latitudes. These studies range from field flux measurements, ecosystem models to satellite measurement analysis. However, the summertime response of the northern vegetation to the summer temperature increase remains uncertain (Angert *et al* 2005, Buermann *et al* 2013, Yi *et al* 2014). Several studies reported the declining trend of summer productivity over boreal ecosystems (Barber *et al* 2000, Angert *et al* 2005, Ma *et al* 2012) and over arctic ecosystems (Sharp *et al* 2013).

Buermann *et al* (2013) reported that earlier spring increases the productivity in North American boreal forests, but also associates drying in the midst of the growing season which decreases summer productivity. Our study is on inter-annual variability for the three summer seasons of 2009–2011, while Buermann *et al* (2013) studied the longer-term climate change impact on boreal forests for nearly three decades (1982–2008). For a long-term period, early spring onset due to global warming trend could result in summer soil moisture and then forest productivity in growing seasons (e.g. Barnett *et al* 2005). On the other hand, this study examined the recent three years, indicating that precipitation in July, immediate past month, impacts the net carbon flux in August. Even the different time span, our finding is consistent with Buermann *et al* (2013) that soil moisture is the key to summertime productivity in boreal forests. On an inter-annual scale, earlier spring onset might not necessarily follow drying of soil moisture. If precipitation in early summer is normal or more than normal, sufficient soil moisture will keep the terrestrial vegetation from drying during the mid-summer so that vegetation productivity could remain or increase. This is the mechanism suggested from joint inversion.

It is interesting to note that the relationship between one-month lagged precipitation anomalies and NDVI reveals a better correlation with the CO_2 flux anomalies from joint inversion than surface inversion, though NDVI alone has a stronger negative correlation with CO_2 fluxes in surface inversion than joint inversion (figure 5). Although NDVI is an indicator of photosynthetic productivity, it is not necessary to be proportional to the net CO_2 flux which is a photosynthetic CO_2 uptake minus respiratory CO_2 release. Positive precipitation anomalies alleviate the water stress of stomata and enhance the photosynthesis (positive NDVI anomaly), leading to the increase of net CO_2 uptake (negative CO_2 flux anomaly). Vice versa is for negative precipitation anomalies. It is interesting that the multiple climate anomalies relationship tells a more comprehensive view on the atmosphere–biosphere CO_2 exchange than with single climate variables.

4.3. Longitudinal distribution of XCO_2 over northern hemisphere

Figure 7 shows the longitudinal distribution of monthly mean XCO_2 north of 60°N with respect to averaged XCO_2 over 40°E–60°E longitude band. The longitude band of 40°E–60°E corresponds to the East Northeastern Europe, and the 60°E–113°E band is to Western Siberia, and the band east of 113°E is to Eastern Siberia, in the present study.

Given the fact that the mean wind is westerly, the relative distribution of XCO_2 reflects the evolution of XCO_2 through CO_2 exchange between the atmosphere and surface along the longitudes. Except 2010, the XCO_2 longitudinal distributions appear to be gradually declining westward or steady as a whole. Such a longitudinal profile is accounted for by weak net CO_2 uptake or almost balanced CO_2 exchange along the longitude. In the summer of 2010, the strong declining trend of XCO_2 from 60°E to 110°E is seen, but XCO_2 is almost steady east of 110°E. This regionally limited declining of XCO_2 trend indicates stronger CO_2 uptake around Western Siberia. Therefore, by constraining the GOSAT XCO_2, joint inversion infers the enhanced net CO_2 uptake in Western Siberia compared in Northeastern Europe and Eastern Siberia. This analysis demonstrates that GOSAT XCO_2 reflects the varying atmosphere-terrestrial biosphere CO_2 exchange on a regional scale.

5. Conclusions

In this study, we examined the inter-annual variability of CO_2 fluxes inferd from GOSAT for three consecutive growing seasons from 2009–2011 in Northern Eurasia (north of ~60°N). The results show the anomalies of CO_2 fluxes from joint inversion with GOSAT XCO_2 and surface CO_2 observations are overall better correlated than surface inversion, with the anomalies of surface temperature, and shortwave radiation. In particular, the estimated CO_2 fluxes by joint inversion show strong correlations with surface temperature in July and August, while no correlation is found with estimated CO_2 fluxes by surface inversion. In 2010, a large part of Eurasia experienced an extremely hot and dry summer though Western Siberia was in cool and wet weather conditions. The estimated CO_2 fluxes with GOSAT XCO_2 show reduced net CO_2 uptake in Northeastern Europe and Eastern Siberia but enhanced net CO_2 uptake in Western Siberia. The opposite weather anomalies among Northern Eurasia can explain these opposite anomalies of estimated regional CO_2 fluxes. Thus, we conclude that GOSAT XCO_2 compensates for the lack of observational coverage by ground-based measurements so as to better capture the varying atmosphere-terrestrial biosphere CO_2 exchange on a regional scale.

The fluxes inferred from GOSAT XCO_2 exhibit a reasonable relationship with precipitation through surface temperature and NDVI anomalies when the one-month time lag of precipitation anomalies to CO_2 flux anomalies is considered. The time lag is accounted for by the processes that the precipitation impacts on surface temperature and NDVI through soil moisture. These results indicate that GOSAT XCO_2 reflects the

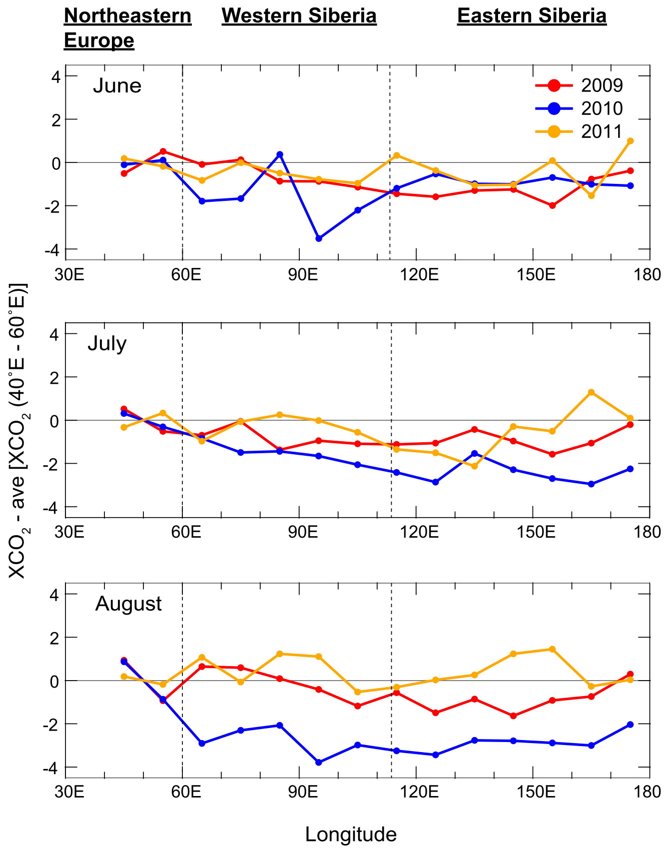

Figure 7. Monthly GOSAT XCO_2 longitudinal distributions with respect to monthly mean XCO_2 over 40°E–60°E over Northeastern Europe region in this study, for June to August 2009–2011. GOSAT XCO_2 are averaged monthly by a 10° longitude band.

combined changes in terrestrial biospheric processes responding to the climate anomalies. In contrast, the anomaly of NDVI alone apparently shows stronger correlation with the fluxes from surface inversion than those from joint inversion. The joint inversion results are more consistent with previous studies claiming the important role of soil moisture under warming climate change on summer productivity over boreal forests. (e.g. Barber *et al* 2000, Angert *et al* 2005, Ma *et al* 2012). The analysis in this study suggests that the inversion performance needs to be evaluated from multiple aspects of climate anomalies, given the complexity in the terrestrial biosphere in time-lagged processes.

Acknowledgments

We would like to thank all colleagues involved the GOSAT project, but in particular, the following people who contributed the developments of atmospheric models and prior flux models: R Zhuravlev, A Ganshin, D Belikov, M Saito, T Oda, and V Valsala. We greatly acknowledge the atmospheric CO_2 data providers of the ObsPack product (obspack_co2_PROTOTYPE_v1.0.3_2013_01-29) that used for the inversion: P Steele, P Krummel, M van der Schoot, L Gatti, A Martinewski, D Worthy, J Hatakka, T Aalto, M Ramonet, M Delmotte, M Schmidt, P Ciais J A Morgui, N Mihalopoulos, F Gheusi, G Bentz, I Levin. S Hammer, L Haszpra, A Takizawa, T Machida, H Matsueda, Y Sawa, S Morimoto, T Nakazawa, S Aoki, H Meijer, E Brunke, E Scheel and C Labushagne, R Ramos, M Leuenberger, S Wofsy, S Biraud. M Torn, K Masarie, A Andrews, E Dlugokencky, C Sweeney, P Tan, K Thoning, B Stephens, R Keeling, A J Gomez-Paleaz, and R Langenfelds. The JCDAS is provided from the Japanese 25-year Reanalysis (JRA-25), a cooperative research project carried out by the Japan Meteorological Agency (JMA) and the Central Research Institute of Electric Power Industry (CRIEPI). The Japanese NDVI and shortwave radiation products are developed by JAXA, using the MODIS and SeaWiFS Level-1 data are provided by NASA GSFC. The authors thank four anonymous reviewers for interesting feedback and helpful comments to improve the manuscript.

References

Angert A, Biraud S, Bonfils C, Henning C C, Buermann W, Pinzon J, Tucker C J and Fung I 2005 Drier summers cancel out the CO_2 uptake enhancement induced by warmer springs *Proc. Natl Acad. Sci. USA* **102** 10823–7

Barber V A, Juday G P and Finney B P 2000 Reduced growth of Alaskan white spruce in the twentieth century from temperature-induced drought stress *Nature* **405** 668–73

Barnett T P, Adam J C and Lettenmaier D P 2005 Potential impacts of a warming climate on water availability in snow-dominated regions *Nature* **438** 303–9
Basu S *et al* 2013 Global CO_2 fluxes estimated from GOSAT retrievals of total column CO_2 *Atmos. Chem. Phys.* **13** 8695–717
Belikov D A *et al* 2013 Simulations of column-averaged CO_2 and CH_4 using the NIES TM with a hybrid sigma-isentropic (σ-θ) vertical coordinate *Atmos. Chem. Phys.* **13** 1713–32
Bruhwiler L M P, Michalak A M, Peters W, Baker D F and Tans P 2005 An improved Kalman Smoother for atmospheric inversions *Atmos. Chem. Phys.* **5** 2691–702
Bruhwiler L M P, Michalak A M and Tans P P 2011 Spatial and temporal resolution of carbon flux estimates for 1983–2002 *Biogeosciences* **8** 1309–31
Buermann W, Bikash P R, Jung M, Burn D H and Reichstein M 2013 Earlier springs decrease peak summer productivity in North American boreal forests *Environ. Res. Lett.* **8** 024027
Chevallier F *et al* 2010 CO_2 surface fluxes at grid point scale estimated from a global 21 year reanalysis of atmospheric measurements *J. Geophys. Res.* **115** D21307
Chevallier F, Maksyutov S, Bousquet P, Bréon F-M, Saito R, Yoshida Y and Yokota T 2009 On the accuracy of the CO_2 surface fluxes to be estimated from the GOSAT observations *Geophys. Res. Lett.* **36** L19807
Chevallier F, Palmer P I, Feng L, Boesch H, O'Dell C W and Bousquet P 2014 Toward robust and consistent regional CO_2 flux estimates from *in situ* and spaceborne measurements of atmospheric CO_2 *Geophys. Res. Lett.* **41** 1065–70
Deng F *et al* 2014 Inferring regional sources and sinks of atmospheric CO_2 from GOSAT XCO_2 data *Atmos. Chem. Phys.* **14** 3703–27
Enting I G 2002 *Inverse Problems in Atmospheric Constituent Transport* (Cambridge, UK: Cambridge University Press)
Enting I G and Newsam G N 1990 Atmospheric constituent inversion problems: Implications for baseline monitoring *J. Atmos. Chem.* **11** 69–87
Ganshin A *et al* 2012 A global coupled Eulerian-Lagrangian model and 1×1 km CO_2 surface flux dataset for high-resolution atmospheric CO_2 transport simulations *Geosci. Model Dev.* **5** 231–43
GLOBALVIEW-CO_2 2011 *Cooperative Atmospheric Data Integration Project -Carbon Doxid.* (Boulder, CO: NOAA ESRL)
Gloor M, Fan S-M, Pacala S and Sarmiento J 2000 Optimal sampling of the atmosphere for purpose of inverse modeling: a model study *Global Biogeochem. Cycles* **14** 407–28
Guerlet S, Basu S, Butz A, Krol M, Hahne P, Houweling S, Hasekamp O P and Aben I 2013 Reduced carbon uptake during the 2010 Northern Hemisphere summer from GOSAT *Geophys. Res. Lett.* **40** 2378–83
Gurney K R *et al* 2004 Transcom 3 inversion intercomparison: Model mean results for the estimation of seasonal carbon sources and sinks *Global Biogeochem. Cycles* **18** GB1010
Houweling S *et al* 2015 An intercomparison of inverse models for estimating sources and sinks of CO_2 using GOSAT measurements *J. Geophys. Res.* **120** 5253–66
Inoue M *et al* 2016 Bias corrections of GOSAT SWIR XCO_2 and XCH_4 with TCCON data and their evaluation using aircraft measurement data *Atmos. Meas. Tech.* **9** 3491–512
Ishizawa M *et al* 2016 Impact of retrieval biases of GOSAT XCO_2 on the surface CO_2 flux estimates (in preparation)
Ito A 2010 Changing ecophysiological processes and carbon budget in East Asian ecosystems under near-future changes in climate: implications for long-term monitoring from a process-based model *J. Plant. Res.* **123** 577–88
Kuze A, Suto H, Nakajima M and Hamazaki T 2009 Thermal and near infrared sensor for carbon observation Fourier-transform spectrometer on the Greenhouse Gases Observing Satellite for greenhouse gases monitoring *Appl. Opt.* **48** 6716–33
Ma Z, Peng C, Zhu Q, Chen H, Yu G, Li W, Zhou X, Wang W and Zhang W 2012 Regional drought-induced reduction in the biomass carbon sink of Canada's boreal forests *Proc. Natl Acad. Sci. USA* **109** 2423–7
Mabuchi K 2013 A numerical study of the relationship between the carbon cycle and the land surface processes in the Northern Hemisphere related to recent El Niño events *J. Meteor. Soc. Japan* **91** 667–86
Mabuchi K, Takagi H and Maksyutov S 2016 Relationships between CO_2 flux estimated by inverse analysis and land surface elements in South America and Africa *J. Meteorol. Soc. Japan* **94** 415–30
Maksyutov S *et al* 2013 Regional CO_2 flux estimates for 2009–2010 based on GOSAT and ground-based CO_2 observations *Atmos. Chem. Phys.* **13** 9351–73
Masarie K A, Peters W, Jacobson A R and Tans P P 2014 ObsPack: a framework for the preparation, delivery, and attribution of atmospheric greenhouse gas measurements *Earth Syst. Sci. Data* **6** 375–84
McGuire A D, Anderson L G, Christensen T R, Dallimore S, Guo L, Hayes D J, Heimann M, Lorenson T D, Macdonald R W and Roulet N 2009 Sensitivity of the carbon cycle in the arctic to climate change *Ecol. Monogr.* **79** 523–55
Myneni R B, Hall G G, Sellers P J and Marshak A L 1995 The interpretation of spectral vegetation indexes *IEEE Trans. Geosci. Remote Sens.* **33** 481–6
Nemani R R, Keeling C D, Hashimoto H, Jolly W M, Piper S C, Tucker C J, Myneni R B and Running S W 2003 Climate-driven increases in global terrestrial net primary production from 1982 to 1999 *Science* **300** 1560 1563
Oda T and Maksyutov S 2011 A very high-resolution (1 km × 1 km) global fossil fuel CO_2 emission inventory derived using a point source database and satellite observations of nighttime lights *Atmos. Chem. Phys.* **11** 543–56
Onogi K *et al* 2007 The JRA-25 Reanalysis *J. Meteor. Soc. Japan* **85** 369–432
Peylin P *et al* 2013 Global atmospheric carbon budget: results from an ensemble of atmospheric CO_2 inversions *Biogeosciences* **10** 6699–720
Rayner P J and O'Brien D M 2001 The utility of remotely sensed CO_2 concentration data in surface source inversions *Geophys. Res. Lett.* **28** 175–8
Reuter M *et al* 2014 Satellite-inferred European carbon sink larger than expected *Atmos. Chem. Phys.* **14** 13739–53
Saeki T *et al* 2013 Inverse modeling of CO_2 fluxes using GOSAT data and multi-year ground-based observations *SOLA* **9** 45–50
Saigusa N *et al* 2010 Impact of meteorological anomalies in the 2003 summer on gross primary productivity in East Asia *Biogeosciences* **7** 641–55
Saito M, Ito A and Maksyutov S 2014 Optimization of a prognostic biosphere model for terrestrial biomass and atmospheric CO_2 variability *Geosci. Model Dev.* **7** 1829–40
Sharp E D, Sullivan P F, Steltzer H, Csank A Z and Welker J M 2013 Complex carbon cycle responses to multi-level warming and supplemental summer rain in the high arctic *Global Change Biol.* **19** 1780–92
Shirai T, Ishizawa M, Zhuravlev R, Ganshin A, Belikov D, Saito M, Oda T, Valsala V and Maksyutov S 2016 A decadal inversion of carbon dioxide using the Global Eulerian-Lagrangian Coupled Atmospheric model (GELCA) *Tellus* submitted
Stohl A, Forster C, Frank A, Seibert P and Wotawa G 2005 Technical note: the lagrangian particle dispersion model FLEXPART version 6.2 *Atmos. Chem. Phys.* **5** 2461–74
Tucker C J 1979 Red and photographic infrared linear combinations for monitoring vegetation *Remote Sens. Environ.* **8** 127–50
Valsala V and Maksyutov S 2010 Simulation and assimilation of global ocean pCO_2 and air-sea CO_2 fluxes using ship observations of surface ocean pCO_2 in a simplified biogeochemical offline model *Tellus* B **62** 821–40
van der Werf G R, Randerson J T, Giglio L, Collatz G J, Mu M, Kasibhatla P S, Morton D C, DeFries R S, Jin Y and van Leeuwen T T 2010 Global fire emissions and the contribution of deforestation, savanna, forest, agricultural, and peat fires (1997–2009) *Atmos. Chem. Phys.* **10** 11707–35

Xie P and Arkin P A 1997 Global precipitation: a 17-year monthly analysis based on gauge observations, satellite estimates, and numerical model outputs *Bull. Am. Meteorol. Soc.* **78** 2539–58

Yi Y, Kimball JS and Reichle R H 2014 Spring hydrology determines summer net carbon uptake in northern ecosystems *Environ. Res. Lett.* **9** 064003

Yoshida Y *et al* 2013 Improvement of the retrieval algorithm for GOSAT SWIR XCO_2 and XCH_4 and their validation using TCCON data *Atmos. Meas. Tech.* **6** 1533–47

Yoshida Y, Ota Y, Eguchi N, Kikuchi N, Nobuta K, Tran H, Morino I and Yokota T 2011 Retrieval algorithm for CO_2 and CH_4 column abundances from short-wavelength infrared spectral observations by the Greenhouse gases observing satellite *Atmos. Meas. Tech.* **4** 717–34

Zimov S A, Davydov S P, Zimova G M, Davydova A I, Schuur E A G, Dutta K and Chapin F S 2006 Permafrost carbon: stock and decomposability of a globally significant carbon pool *Geophys. Res. Lett.* **33** L20502